Biomedicine & Pharmacotherapy 165 (2023) 115156

Contents lists available at ScienceDirect

Biomedicine & Pharmacotherapy

journal homepage: www.elsevier.com/locate/biopha

A calcium peroxide incorporated oxygen releasing chitosan-PVA patch for Diabetic wound healing

Asad Ullah [a,b], Abdulla Al Mamun [a,b], Midhat Batool Zaidi [c], Talat Roome [c,d], Anwarul Hasan [a,b,*]

[a] Department of Mechanical and Industrial Engineering, Qatar university, Qatar
[b] Biomedical Research Center, Qatar University, Qatar
[c] Dow Institute for Advanced Biological and Animal Research, Dow International Medical College, Dow University of Health Sciences, Qatar
[d] Molecular Pathology Section, Department of Pathology, Dow Diagnostic Reference and Research Laboratory, Dow University of Health Sciences, Qatar

ARTICLE INFO

Keywords:
Diabetic wound healing
Chronic hypoxia
Oxygen releasing materials

ABSTRACT

Impaired wound healing is a major healthcare problem in patients with diabetes often resulting in gangrene, microbial infection and amputation of affected limb. The delay or absence in healing process arises from several abnormalities, among them chronic hypoxia is a major concern due to its associated issues such as lack of collagen deposition, epithelization, fibroplasia, angiogenesis, and resistance to infections at the wound site. To address hypoxia, delivery of oxygen at the wound site through oxygen releasing agents have been proven to be effective therapeutics. Several oxygen releasing nanoparticles such as Sodium Percarbonate (SPC), Calcium Peroxide (CPO), Hydrogen Peroxide, Magnesium Peroxide (MPO) have been investigated in wound healing application. However, the uncontrolled/burst release of these nanotherapeutic agents and its accompanied cytotoxicity pose a barrier in expediting the healing process. In this study, a Chitosan-Polyvinyl alcohol (CS-PVA) based hydrogel containing oxygen releasing nanoparticle, calcium peroxide (CPO) was constructed to provide a slow and sustained delivery of oxygen for at least 5 days. In-vitro cell culture studies with this material using fibroblast and endothelial cell line exhibited improved biocompatibility, cell viability and enhanced proliferation in comparison with the control group. Additionally, cell migration study using scratch assay method showed superior cell migration ability of our proposed materials. Furthermore, In vivo study using diabetic rat model showed accelerated wound closure rate compared to untreated control wounds.

1. Introduction

Diabetes currently affects more than 400 million people globally, and by 2045, that number will rise to about 629 million [1]. Due to the rising incidence of diabetes mellitus worldwide, complications like chronic wounds have emerged as serious issues that endanger patients' health and quality of life [2]. Chronic wounds, such as diabetic foot ulcers, are more likely to occur in diabetes patients—more than 20% more likely [3]. For patients with diabetes, such chronicity can have serious consequences because chronic wounds seem to be the main reason for diabetes-related amputations [4]. For instance, 14–24% of patients with diabetic foot ulcers (DFUs) must have their lower extremities amputated as a result of the complication, which is a risky and life-changing treatment with a 5-year death rate of about 50–59% [5]. Thus, the development regarding effective/curative care for chronic wounds has emerged as a crucial clinical challenge for researchers [6].

The wound healing process consists of inflammation, proliferation, and remodeling, with various cells, cytokines, and growth factors orchestrating each stage for successful healing [7]. However, in diabetes, alterations in biological and cellular factors lead to chronic inflammation, hindering the healing process [8,9]. Diabetic wounds face multiple challenges, including chronic hypoxia, inadequate angiogenesis, impaired antimicrobial activity, increased interactions between endothelial cells and leukocytes, and compromised functionality of neutrophils in a hyperglycemic environment [10-12]. Chronic hypoxia is particularly noteworthy as it hampers crucial aspects of wound healing, such as collagen deposition, epithelization, fibroplasia, angiogenesis, and resistance to infection, due to insufficient oxygen and nutrient supply to the regenerating tissue [13,14].

Various oxygen therapies, such as hyperbaric oxygen therapy (HBOT) and topical gaseous oxygen therapy (TGO), have been explored to address chronic hypoxia and aid in the healing process of chronic

* Correspondence to: P.O. Box:2713, University Street, Doha, Qatar.
E-mail address: hasan.anwarul.mit@gmail.com (A. Hasan).

https://doi.org/10.1016/j.biopha.2023.115156
Received 23 May 2023; Received in revised form 6 July 2023; Accepted 11 July 2023
Available online 2 August 2023

wounds [10,15,16]. HBOT, delivering supplemental 100% oxygen at increased pressure [17], has shown potential in promoting angiogenesis, reducing edema, and enhancing tissue development [18,19]. TGO, an alternative to HBOT, offers practicality and fewer complications. However, both therapies have limitations in sustaining adequate oxygen levels for wounds, and their efficacy has shown mixed results [20-22]. For instance, Oxygen levels are only temporarily elevated during therapy before returning to baseline shortly after discontinuation [22-24].

In order to provide sustainable oxygen level over a long period of time, oxygen releasing materials(ORMs) has been a widely accepted norm in tissue engineering [25,26]. Oxygen-releasing biomaterials can be created by incorporating oxygen generating materials (OGMs) such as solid peroxides, liquid peroxides, and fluorinated chemicals into the hydrogels [26]. Sodium percarbonate (SPC), calcium peroxide (CPO), magnesium peroxide (MPO), hydrogen peroxide (HPO) are the most frequent peroxides used in tissue engineering. However, liquid peroxides like HPO disintegrates immediately into oxygen molecules [27]. As a result, persistent oxygen release is more susceptible with solid peroxides (CPO, MPO, SPC) than with liquid peroxides [28]. However, calcium peroxide (CPO) is favored among other solid peroxides for two reasons: 1) CPO's oxygen generation is sustained and slower than SPC, and 2) highly pure CPO can be obtained commercially than MPO [29]. As a result, CPO is regarded as one of the most reliable OGMs in biomedical applications, notably for the release of Ca^{2+} ions that may be helpful to the function of tissues or organs (e.g., bone and heart) [28,30]. However, during the disintegration process of Calcium Peroxide (CPO) for oxygen production, an intermediary product, hydrogen peroxide, is generated [31]. Excessive hydrogen peroxide levels can be cytotoxic, harming nearby tissues. Furthermore, elevated levels of reactive oxygen species (ROS) stemming from hydrogen peroxide can interact with cellular lipids, proteins, and DNA, resulting in cellular damage and demise [32]. Therefore, caution must be exercised to prevent these negative consequences specially related to burst release.

To control the burst release of oxygen, polymeric encapsulation of these OGMs can be a viable option. Different OGMs are being encapsulated in polymers in order to fabricate wound dressing patch which can release oxygen up to several days [33]. Hydrogel dressings recently gained prominence due to its ability to reestablish wound-friendly microenvironments, such as by keeping the skin hydrated, soaking up tissue exudates, enabling oxygen penetration, lowering inflammation, and perhaps adjusting local immunogenicity [34]. Chitosan (CS), a prominent constituent of these hydrogels, is widely employed in the medical area due to features such as biodegradability and biocompatibility [35]. However, chitosan has limited mechanical properties, and a simple solution is to combine it with various polymeric materials such as Polyvinyl alcohol (PVA) [36]. PVA is a potential polymeric material with a number of intriguing features, including biocompatibility, high hydrophilicity and nontoxicity, and it is commonly used to make hydrogels for biomedical purposes [37].

This Chitosan-PVA blend is a proven candidate in wound healing applications. The current project's goal was to create an oxygen-releasing calcium peroxide incorporated CS-PVA hydrogel patch to combat hypoxia related issues by combining biocompatible and biodegradable polymers like CS and PVA crosslinked with a crosslinker [38,39]. CS was chosen due to its proliferative activity and antibacterial properties which will aid the healing process and PVA was selected to increase the hydrogel's mechanical strength.

2. Material and methods

2.1. Materials

Santa Cruz Biotechnology USA provided CS with a molecular weight of 20 kDa, PVA (fully hydrolyzed and molecular weight 57–66 kDa) and 5% glutaraldehyde solution. Gibco Technologies, USA, provided Dulbecco's modified Eagle's medium (DMEM), fetal bovine serum (FBS), phosphate buffered saline (PBS) of pH 7.4, 0.2% trypsin-EDTA, and penicillin/streptomycin. Invitrogen biotechnology provided a cell staining kit for live/dead imaging. Sigma-Aldrich USA supplied the dimethyl sulfoxide (DMSO) and Thermo Fisher Scientific provided with the MTT (3-(4,5-Dimethylthiazol-2-yl)− 2,5-Diphenyltetrazolium Bromide) dye.

2.2. Fabrication of CPO embedded CS-PVA hydrogel

To develop CS-PVA blend, a solution of 3% chitosan (CS) in a 0.5 molar glacial acetic acid was formed. The pH of the mixture was measured and 1 molar sodium hydroxide solution was added dropwise to the solution to adjust the pH at around 6. This solution was kept in a refrigerator at 4 °C for later usage. Similarly, 10% (w/v) PVA solution was produced in deionized water by keeping the solution under constant stirring at around 80 °C. Both CS and PVA solution was mixed at a ratio of 1:1 and was kept under constant stirring for 1 h to produce a homogeneous mixture. After mixing the blend, the crosslinking agent, glutaraldehyde (2% v/v) was added dropwise to the polymeric blend under constant stirring. After 30 min, the solution of around 5 ml was poured into centrifuge tubes. Later on, different concentrations of oxygen releasing nanoparticle, CPO were added into the solution and were vortex mixed and sonicated for 40 min properly to homogenously disperse the nanoparticles throughout the solution. The sonicated solutions were poured into a petri dish and freeze-thaw cycle were performed two times to crosslink the polymeric blend to develop the hydrogels. Using this method blank CS-PVA, 0.5 mg/ml and 1 mg/ml CPO contained CS-PVA hydrogels were formed and kept at 4 °C for better storage.

2.3. Physical Characterization of The Developed Patch

2.3.1. Scanning electron microscopy (SEM)

To determine the surface topography and composition of the hydrogel samples, a scanning electron microscopy technique was utilized using a SEM (Nova Nano SEM 450). The samples were sliced with an 8 mm biopsy punch, and adhered to the stubs with double-sided adhesive tape.

2.3.2. Energy-dispersive X-ray spectroscopy (EDX)

EDX spectroscopy was utilized to observe the incorporation of oxygen releasing agent (CPO) in the hydrogel samples. The energy distributions and intensity of the X-ray signal generated by a focused electron beam on the sample were measured and counted. When X-ray photons dispersed over the detector, the signals were displayed on the display, revealing the respective peaks of different constituent present in hydrogel samples.

2.3.3. Fourier transform infrared spectroscopy (FTIR)

FTIR spectroscopy was utilized to analyze the chemical composition of CS-PVA hydrogels loaded with CPO. The FTIR spectra of CS, PVA, CS-PVA, CPO, and different concentration of CPO contained CS-PVA hydrogels were determined using samples weight of roughly 10 mg. The FTIR absorbance peaks were measured using the PerkinElmer (USA) Spectrum 400.

2.4. Swelling study

The gravimetric approach was used to evaluate the swelling characteristics of CS-PVA hydrogel and nanocomposite hydrogels (CS-PVA-CPO). The desiccated materials were first weighed (W_{dry}) before being put in petri plates filled with PBS. The petri plates were then fixed in a water bath under constant temperature. Finally, the samples were extracted and weighed at various time periods. The samples were wiped with filter paper to remove excess solvent before weighing. Eq. 1 was then used to compute the swelling characteristics.

$$\frac{(Weight\ of\ hydrogel\ sample\ after\ time, t - weight\ of\ initial\ dry\ hydrogel)}{(weight\ of\ initial\ dry\ hydrogel)} \times 100 \quad (1)$$

2.5. Release study

Release of oxygen from fabricated CS-PVA-CPO hydrogels was measure using "Presens Oxygen microsensor". This study had been investigated in PBS. Calcium peroxide nanoparticles containing CS-PVA hydrogels and blank CS-PVA were kept in a tube filled with 1 ml of PBS at room temperature. At a specific interval of one day, small amount of PBS (100 μl) withdrawn from the tube and read using the oxygen microsensor. The withdrawn sample then put back into the original solution.

2.6. Porosity study

The porosity of the scaffolds was determined using the mass method with ethanol as the displacement liquid. Initially, the dry weight of the scaffolds (W) was measured. Subsequently, the scaffolds were immersed in a known volume of ethanol (V1) for a duration of 10 min. The total volume of ethanol, denoted as V2, was recorded after impregnation into the scaffolds. Following this, the ethanol-impregnated scaffolds were removed from the cylinder, and the remaining volume of ethanol (V3) was measured. The porosity percentage (P) of the scaffolds was obtained by the following equation

$$Porosity, P = \frac{V_1 - V_3}{V_2 - V_3} \quad (2)$$

2.7. Biological characterization

2.7.1. Live/dead assay

Live/Dead assay is a very popular technique to assess the cell viability and cell cytotoxicity. In this experiment, this assay was used to measure the effect of our fabricated hydrogels on the viability of fibroblast and endothelial cells. The cells were seeded with a density of 50×10^3 cells/well in a 24 well microplates. After the incubation of 24 h, hydrogels sample were added into the microplates. The plates were removed from the incubator after 1 and 3 days and all the samples and media were removed. After washing each well with DPBS, 100 μl of prepared Live/Dead assay was added and incubated for 30 min. After 30 min of incubation, the images of the plates were captured using a fluorescent microscope.

2.7.2. Scratch assay

To assess the In vitro wound healing, scratch assay was utilized. Fibroblast and endothelial cells were seeded into a 12 well plate. The seeding density was kept 100×10^3 cells/well. Upon reaching the 90% confluency, the plates were scratched using the tip of 100 μl pipette tip and washed in DPBS. After that the image of the scratch was taken using a microscope. After taking the image, prepared samples were added into the well plates and kept in incubator for 24 h. At the end of the incubation period, the samples were taken out from the plates and again the image of the scratch was taken from the microscope. Wound contractions were calculated using the ImageJ software.

2.7.3. MTT assay

The MTT test, a colorimetric assay, is used to assess cell viability, cell cytotoxicity and proliferation by measuring cell's metabolic activity. This assay was used to measure the cell proliferation rate of our fabricated CS-PVA and CS-PVA-CPO hydrogels. In this experiment, 3T3 fibroblasts and endothelial cells (EA.hy926) were seeded into a 24 well microplates followed by the addition of hydrogels samples. The seeding density of these cells were 50×10^3 cells/well. The microplates were taken out from the incubator at 1,2,3 days of incubation period. Then after taking out of the hydrogel samples, old media was replaced by fresh media of 400 μl. This followed by the addition of 100 μl of MTT dye in each plate and incubation for 3 h. After 3 h, the supernatants were discarded and 300 μl of DMSO were added to make the formazan crystal dissolve. The media were transferred into a 96 well plate with a volume of 100 μl per well. The 96 well plate was read using a microplate reader at 570 nm and cell proliferation rate were calculated using the formula stated below.

$$\text{Cell proliferation rate}(\%) = (\text{OD of Sample}/\text{OD of Control}) \times 100 \quad (3)$$

2.8. Animal studies

2.8.1. Experimental animals

In-house–bred, albino, Wistar strain rats of either gender weighting 150 gm were obtained from Central Animal House, Dow Institute for Advanced Biological and Animal Research (DIABAR), Dow University of Health Sciences (DUHS). Rats were distributed into treated and untreated/control groups (n = 6), housed in a controlled environment of 21 ± 1°C, with a 12-hour light-dark cycle and 55 ± 5% relative humidity of Advanced Research Laboratory (ARL). During the study period, the experimental rats were provided with a standard chow diet and water ad libitum. The experiments were performed under the guidance and approval of the Institutional Animal Care and Use Committee (IACUC), DUHS.

2.8.2. Wound model

Through the adoption of existing techniques described in literature, hyperglycemia was induced in Wistar strain rats [40]. Before surgical operations, general anesthesia was administered intraperitoneally with a mixture of xylazine (7 mg/kg) and ketamine (60 mg/kg). Before generating wounds, the rats' dorsal surfaces were shaved with a sterile razor while they were anesthetized. The dorsal region was disinfected with povidone-iodine. On the dorsal shaved area, a full-thickness 2 cm wound was made. Each animal's wounds were treated with CS-PVA-CPO-0.5 patches and normal saline (control) before being wrapped with basic surgical tapes.

2.8.3. Macroscopic healing assessment

The wound size was observed daily, and the animals were meticulously watched until the 14-day study period. The wound closure (in percentage of the original wound) was estimated in the same way that it has been reported in the literature. Briefly, the healing was recorded and captured every 3rd day post-wound induction and wound area closure was measured and calculated the by applying the given formula:

(Original wound area - Actual wound area) / (Original wound area) × 100(4)

2.8.4. Histological assessments

On day 3, 6, 9, and 14, surgical samples of healed skin tissue were taken and fixed in 4% PFA for 24 h at room temperature. The sampled tissues, after appropriate fixation in formalin were then processed for embedding into paraffin wax. The 5 micrometer sections of sampled tissue were collected on slides and further stained following standard hematoxylin and eosin (H&E) staining. Briefly, these sections were dewaxed, dehydrated, and stained with hematoxylin. Later, differentiated by mild acid, blued by treatment of weakly alkaline solution, then stained with eosin, re-dehydrated, cleared, mounted, and covered with cover-slip. The images were then acquired using an Olympus light microscope.

2.9. statistical analysis

Each type of experiment was conducted three times, and results were

expressed as the mean and standard deviation (SD). A statistical, Minitab, software was used to run the t-test and ANOVA between various groups. Statistical significance was defined as a p-value less than 0.05.

3. Results and discussion

In this study, an oxygen releasing diabetic wound healing hydrogel patch has been synthesized using chitosan and PVA as carrier materials and CPO NPs as oxygen donor. The primary hypothesis was to combat the hypoxia related issues associated with chronic and diabetic wounds, which in turn will facilitate wound healing. Several challenges were faced during the incorporation of the O2 donor such as, distribution of the NPs in the hydrogel matrix, concentration of the NPs, and size and thickness of the hydrogel patch. Furthermore, due to the high molecular weight and viscosity of CS-PVA, the polymeric solution was required to be sonicated for a longer duration after addition of CPO NPs to well disperse the NPs in the solution. The optimized concentration of CPO NPs was optimized using in vitro studies and CPO with 0.5 mg/ml of CS-PVA solution was been used in this study as an optimized concentration of O_2 donor.

3.1. Morphology of samples

Fig. 1(A-C) depicts morphology of the surface of CS-PVA, CS-PVA-CPO-0.5, and CS-PVA-CPO-1 hydrogel samples. As shown in the figure, the synthesized hydrogels feature a porous structure, which is one of the excellent traits for the regulated release of payload in an ambient environment41. Furthermore, the number of pores increased as the concentration/amount of CPO increased. This increased number of pores might be attributed to pre-release of oxygen from CPO while loading the nanoparticles inside CS-PVA hydrogels.

3.2. EDX analysis

EDX spectroscopy was employed in order to validate the presence of CPO in the CS-PVA hydrogel. The EDX spectra of hydrogel samples of blank CS-PVA and CS-PVA containing CPO NPs are shown in Fig. 1(D-F). The EDX peaks confirm that carbon, oxygen, and calcium were present in the hydrogel samples. Absence of calcium peak confirmed the absence of calcium peroxide in blank CS-PVA hydrogel (Fig. 1D). however, Figs. 1E and 1F shows subsequent peaks of calcium to confirm the incorporation of CPO inside CS-PVA hydrogel. Furthermore, the higher content of oxygen and calcium in CS-PVA-CPO-1 (Fig. 1F) confirmed the higher quantity of CPO compared with CS-PVA-CPO-0.5 (Fig. 1E).

3.3. FTIR

FTIR was utilized to identify the functional groups of CS, PVA, CS-PVA, CPO and CS-PVA containing CPO NPs as given in Fig. 2A. For the pure chitosan the peaks at 1066 and 1018 cm^{-1} corresponds to the starching vibration of C-O and the peak at 1400 cm^{-1} shows the symmetrical vibration of CH_3. The bands at 3350 cm^{-1} exhibit the secondary amine group (NH) and OH, which is present for all the hydrogel samples and the absorption band at 2900 cm^{-1} gives the stretching vibration of C-H. The absorption bands at 3500 and 2900 cm^{-1} show the presence of alkyl groups in chitosan. For the pure PVA, the peaks at 1600 and 1700 cm^{-1} represent the acetate structure with the stretch vibration of C═O and C-O. The absorbance peaks at 700 and 500 cm^{-1} show the

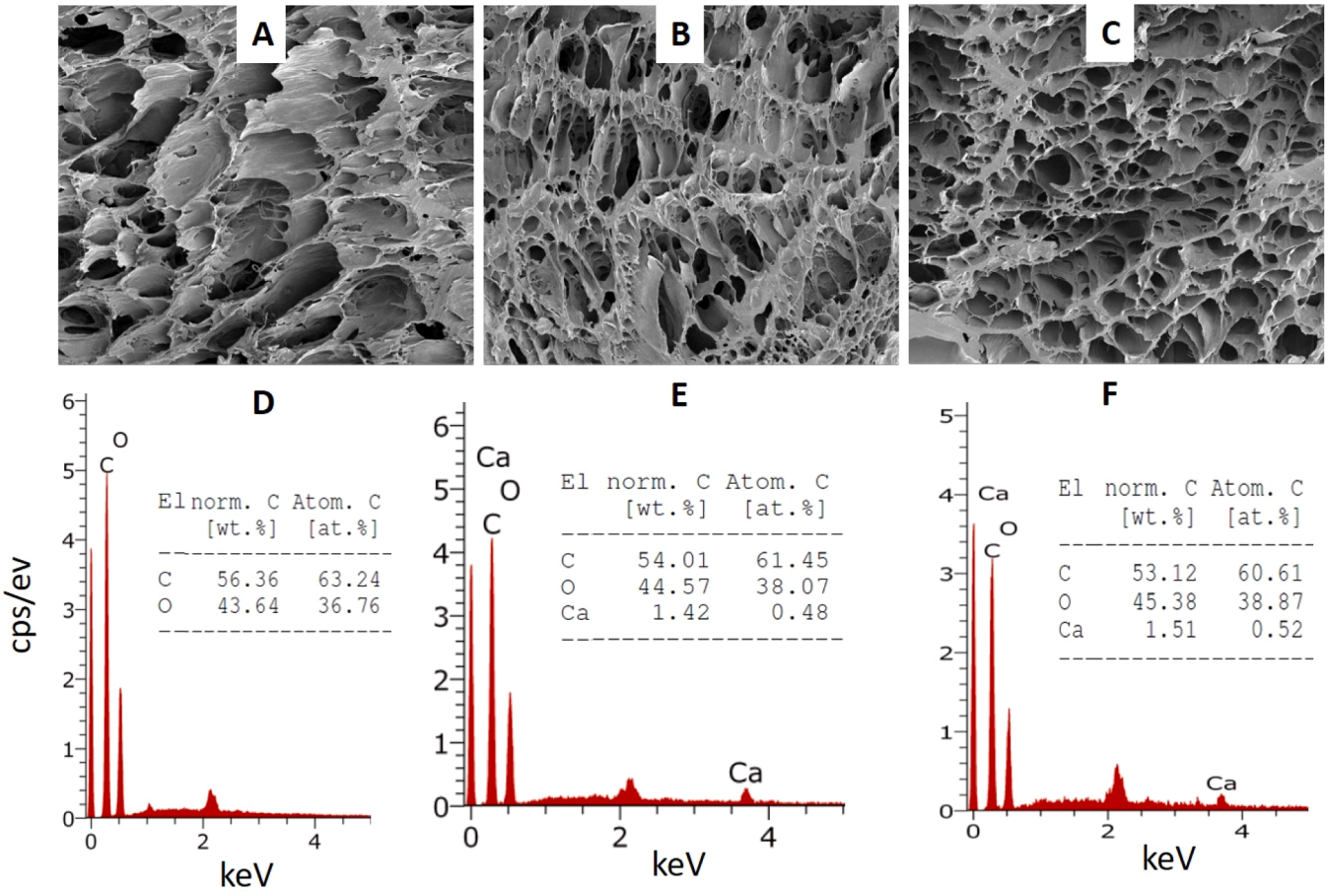

Fig. 1. Characterization of Oxygen releasing patches. Scanning electron microscopic images of CS-PVA and CPO containing CS-PVA hydrogels (A-C). Energy Dispersive X-Ray Analysis of proposed CS-PVA and CPO containing CS-PVA hydrogels to confirm the incorporation of CPO in CS-PVA (D-F).

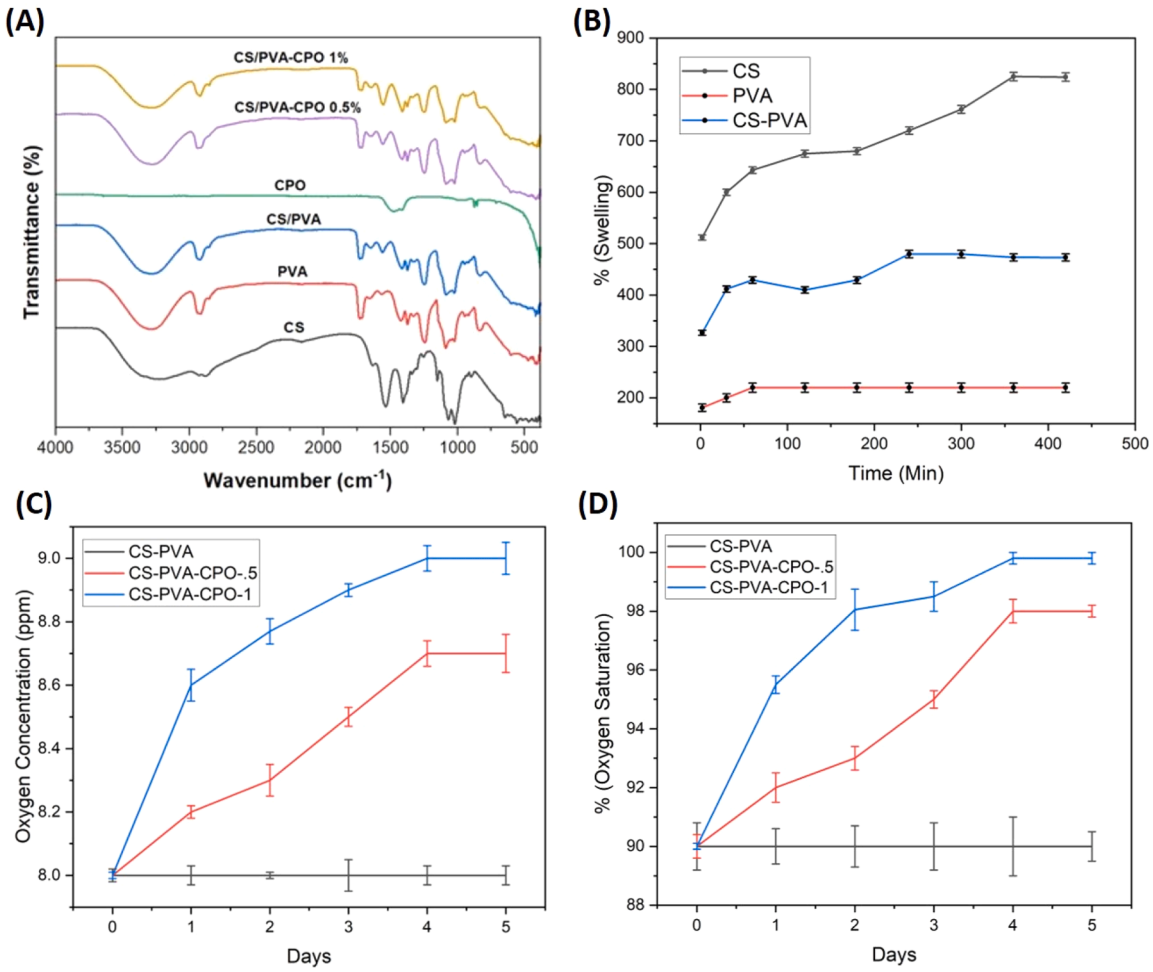

Fig. 2. FTIR curve of CS, PVA, blank CS-PVA, CPO and CPO containing CS-PVA (A). Swelling characteristics of CS, PVA and blank CS-PVA over the period of 7 hr or 420 min (B). Changes in the amount of dissolved oxygen and oxygen saturation as a result of oxygen release from CPO containing CS-PVA hydrogels (C&D).

stretching vibration of O-O and O-Ca-O respectively. These peaks are also evident in CS-PVA samples containing CPO. Thus, the FTIR spectrum shown in Fig. 2A confirms the successful incorporation of CPO NPs into the hydrogels.

3.4. Swelling behavior

The hydrogel can capture wound exudate and offer a moist environment to aid in the healing process [41]. Thus, the water retention or swelling behavior of hydrogel is important in wound healing application. To examine the swelling performance, hydrogel samples of CS, PVA and CS-PVA were put in PBS solution at 37^0 C. Fig. 2B shows the swelling behavior of the given hydrogels.

PVA showed least amount of swelling with a swelling percentage of around 220% within 50 min of immersion. On the other hand, Chitosan (CS) demonstrated highest swelling ability of more than 800% after immersion of around 7 hr or 420 min. As CS-PVA is actually a blend of both CS and PVA, it showed intermediate swelling ability with a percentage of more than 450%. Furthermore, because added nanoparticles were in a small quantity, it was assumed that addition of nanoparticles didn't influence the swelling properties of CS-PVA significantly.

3.5. O_2 Release profile

Amount of dissolved oxygen and percentage of oxygen saturation of PBS solution containing oxygen releasing hydrogels were adopted to verify the release of oxygen from CPO embedded CS-PVA hydrogel samples. The experiment was conducted for 5 days to observe the subtle and persistent release of oxygen from the nanocomposite-based hydrogel (Fig. 2(C&D)). Blank CS-PVA immersed PBS solution showed a steady level of dissolved oxygen (8 ppm) indicating no-release of oxygen in PBS solution. However, immersion of CS-PVA-CPO in PBS solution increased the amount of dissolved oxygen as well as oxygen saturation percentage. CS-PVA-CPO-1 hydrogel showed superior release profile compared to CS-PVA-CPO-0.5 due to higher concentration of embedded CPO nanoparticles.

For CS-PVA-CPO-1, Starting from 8 ppm, oxygen level rose to around 8.6 ppm which corresponds to around 95% oxygen saturation after day 1. Level of oxygen increased slowly and reached a peak value of around 9 ppm or 100% oxygen saturation at day 4. After that, the level of oxygen remained same as the solution was already saturated. Additionally, CS-PVA-CPO-0.5 showed a slow and steady release profile and reached around 97% oxygen saturation at day 4. Furthermore, the amount of released oxygen from CS-PVA-CPO-0.5 was lower at each day when compared with 1% (w/v) CPO loaded CS-PVA hydrogel.

3.6. Porosity study

Glutaraldehyde cross-linking was employed to create pores in the hydrogel films. Porosity of the hydrogel loaded without and with 0.5 mg/ml CPO were determined to be around 0.667 and 0.695, respectively. Adding additional CPO did not significantly increase the porosity of the prepared patch. These values indicate that the resulting hydrogel possesses a porous and cellular structure. Furthermore,

addition of calcium peroxide further increased the porosity which might be attributed to pre-release of oxygen from the scaffolds. These observations are consistent with the findings from the SEM analysis depicted in Fig. 1.

3.7. Live/dead assay

Although oxygen releasing agents have potential to faster the healing process by minimizing hypoxia related issues, several articles have demonstrated its dose dependent cytotoxic effects on different cell lines [42]. With a view to visualizing the cytotoxicity of our fabricated patch on two different cell line, Fibroblast (3T3) and endothelial (EA.hy926), live/dead assay was performed. The state of the distribution of live and dead cells on two different cell lines can be observed in Fig. 3A.

In 3T3 cell line, control group, hydrogel (CS-PVA) and CPO containing hydrogel exhibited almost similar effects with minimal

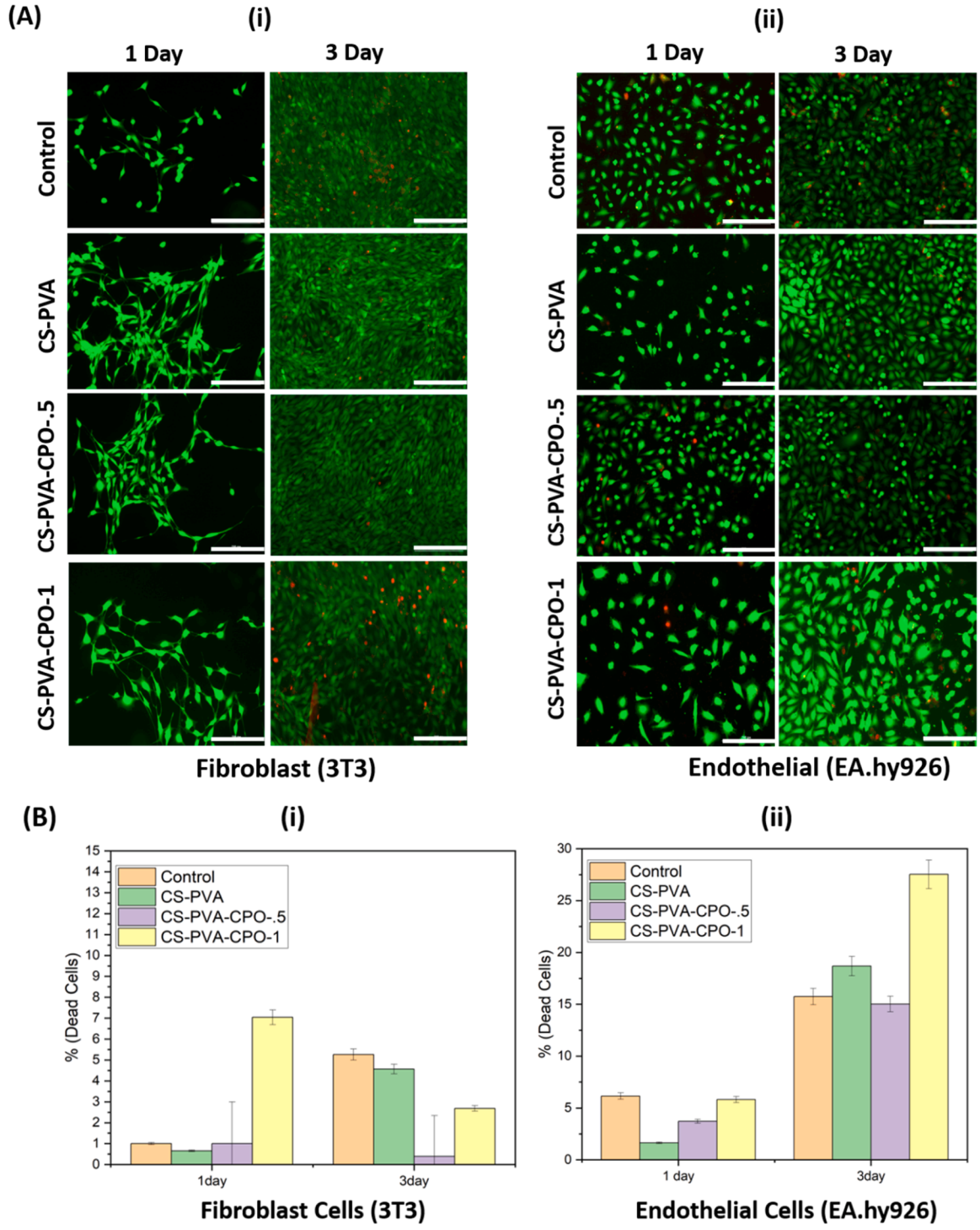

Fig. 3. Live dead assay of oxygen releasing patches using fibroblast and endothelial cell lines. (A) Fluorescence images after performing Live/Dead assay. (i) Images from fibroblast (3T3) cell lines. Green dots depict the live cells while the red dots illustrate dead cells. (ii) Images from endothelial (EA.hy926) cell lines. Green dots depict the live cells while the red dots illustrate dead cells. (B) analysis of fluorescence images using ImageJ software. (i) comparison of the percentage of dead cells among different groups on Fibroblast (3T3) cell line. (ii) comparison of the percentage of dead cells among different groups on endothelial (EA.hy926) cell line. The white scale bar at the right lower corner is 1000 μm.

cytotoxicity (Fig. 3A(i)). Images analyzed using ImageJ to quantify the ratio of live and dead cells showed almost identical distribution of dead cells (around 1–2%) for up to 0.5% (w/v) CPO (Fig. 3B(i)). Percentage of dead cells or cytotoxicity of CPO containing hydrogel increased at the concentration level of 1% w/v after 1 day of incubation. However, cytotoxicity of the same patch containing 1% w/v of CPO didn't show significant difference with other groups after an incubation period of 3 days. Similarly, in endothelial cell line, live cells (green) outnumbered the dead cells (read) in all groups (Fig. 3A(ii)). However, after incubating for 3 days, hydrogels containing 1% w/v CPO showed significant cytotoxic effect compared to other groups (Fig. 3B(ii)).

Overall, results illustrated that, calcium peroxide up to 0.5% w/v CPO didn't have any significant cytotoxic effects in both cell lines. However, increasing the concentration of CPO might induce significant

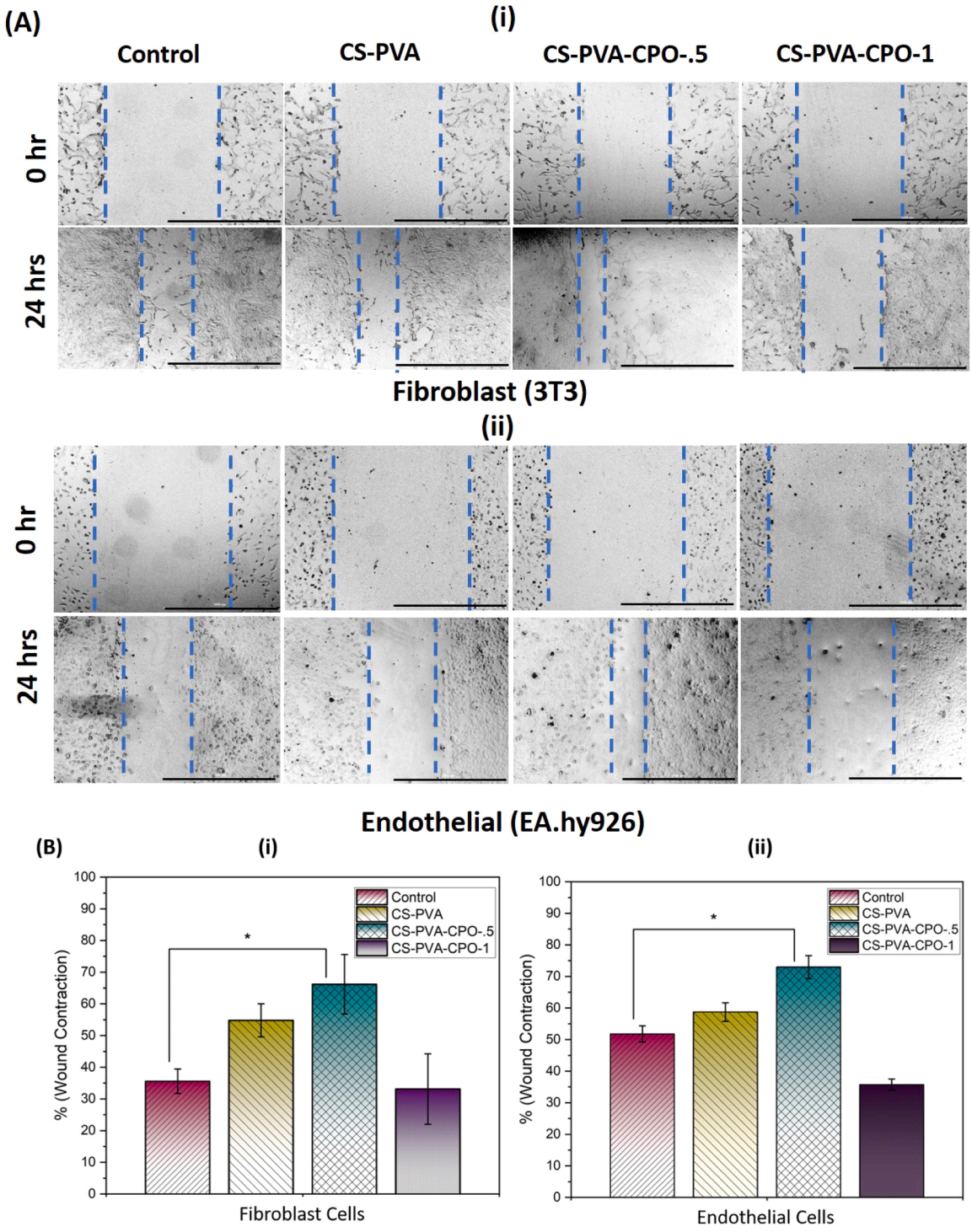

Fig. 4. scratch/migration assay of oxygen releasing patches using fibroblast and endothelial cell lines. Visual representation of Cell migration after performing Scratch assay (A). Images obtained from fibroblast (3T3) cell lines (i). Images obtained from endothelial (EA.hy926) cell lines (ii). Quantitative analysis of cell migration using ImageJ software (B). Comparison of cell migration ability among different groups of hydrogels on Fibroblast (3T3) cell line (i). Comparison of cell migration ability among different groups of hydrogels on endothelial (EA.hy926) cell line (ii). The black scale bar at the right lower corner is 1000 μm. All studies were carried out in triplicate, with a p-value of * $P < 0.05$.

toxicity on cells viability.

3.8. Scratch assay

To investigate the impact of CPO incorporated CS-PVA patch on wound healing, a dose dependent experiment had been carried using fibroblast (3T3) and endothelial (EA.hy926) cell lines. Fig. 4 illustrated both qualitative and quantitative results obtained from scratch assay. In fibroblast cell, CS-PVA hydrogels showed higher wound healing rate compared to untreated control group. Additionally, incorporation of CPO (0.5 mg/ml) enhanced the wound healing potential of the fabricated patch. However, further increasing the concentration of CPO showed negative effect and reduced the healing ability significantly (Fig. 4 A(i)). Similarly, quantitative analysis using ImageJ software showed wound contraction of CS-PVA-CPO-0.5 almost twice as high as with untreated control group (Fig. 4B(i)).

Experiment carried out with endothelial cell line exhibited almost similar effect. Blank CS-PVA hydrogel showed enhanced wound healing than control group. Delivery of oxygen through CPO further increased the rate considerably up to a concentration of 0.5 mg/ml. however, a further increase showed detrimental effect on wound contraction (Fig. 4 A(ii)). Furthermore, quantitative data analysis showed a dose-dependent response of our fabricated patch. CPO incorporated at 0.5 mg/ml showed statistically significant increase in healing activity compared with other groups.

In brief, both qualitative and quantitative analysis corroborate the enhanced In vitro wound healing rate of 0.5 mg/ml CPO incorporated CS-PVA hydrogels (CS-PVA-CPO-0.5) on fibroblast and endothelial cell lines.

3.9. Cell proliferation assay

In order to study the relative proliferation of cultured fibroblast and endothelial cells on control, blank hydrogels and oxygen releasing nanoparticle embedded hydrogels, MTT assay were conducted after 1 day, 2 days and 3 days of culture period. Results demonstrated an increased rate of proliferation of 3T3 fibroblast cells with time for CS-PVA-CPO-0.5. However, a decreased rate of proliferation over the given time period of 3 days was observed for CS-PVA-CPO-1 (Fig. 5 A). Similarly, results obtained from MTT assay of cultured EA.hy926 endothelial cells on our fabricated CPO loaded CS-PVA hydrogel demonstrated an increased rate of relative proliferation with time for CS-PVA-CPO-0.5. Unlike 3T3 fibroblast cells, CS-PVA-CPO-1 induced proliferation rate increased over the given time period of 3 days (Fig. 5B).

The findings of in vitro cell culture study revealed that relative cell proliferation with respect to control group was concentration dependent. The increased CPO levels might have reduced cell growth in comparison with lower concentration. As a result, the strongest candidate for facilitating the healing of chronic wounds may be the optimal concentration of hydrogel, such as the composition of CS-PVA-CPO-0.5 hydrogels.

3.10. Animal studies

The in vivo healing potential of a CPO-incorporated CS-PVA patch when applied directly to a wounded spot was evaluated on wistar rats, and the findings are shown in Fig. 5. On the very first day of the investigation, the wound site of the rats showed bruising, mild bleeding, and epithelial damage produced by the excision (Fig. 6A). However, on the third day, there were symptoms of inflammation and the dermis seemed to be somewhat necrotic. The wound area shrank significantly in all groups, with the CS-PVA-CPO-0.5 patch causing the most shrinkage. Furthermore, fresh hair growth was noticed over the healed regions around the borders of the lesion. The hair development on the CS-PVA-CPO-0.5 group might be attributed to the repair of the undamaged epidermis and dermis. However, among all treatment groups, the un-treated wounds had the least amount of hair growth.

The wound contraction percentage was also estimated to assess the amount of healing of the wound, and the results are shown in Fig. 6B. The significantly increased wound closure was noted from day 3 onwards in treated wound as compared to un-treated wounds. This showed promising wound healing efficacy of oxygen released from the CS-PVA-CPO-0.5 patch. On the final day of the study (14th day), the wound site treated with the CS-PVA-CPO-0.5 patch showed more than 10% more profound reduction in wound margin compared to un-treated control. CS-PVA-CPO-0.5 patch treated group recovered and healed with the regular dermal tissue and hair growth all around the wound area leaving only a light mark. Conversely, the control group did not heal completely exposing a considerable unhealed region with reduced fur.

The microscopic analysis (observed at 10X and 20X magnification) complemented the macroscopic findings, covering the phases of healing inflammation, proliferation and remodeling (Fig. 6C & Fig. 7). The H&E stained tissue sections of day 3 treated groups when observed under

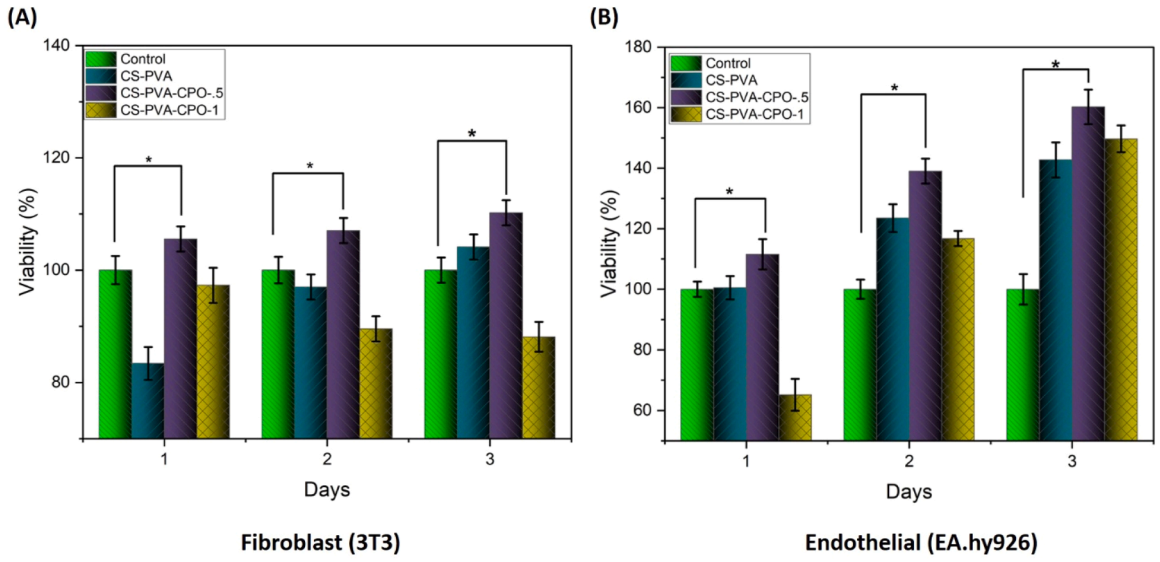

Fig. 5. (A-B) shows the MTT assay results of control and hydrogel patches using fibroblast (A) and endothelial (B) cell lines for 1,2 and 3 days. All studies were carried out in triplicate, with a p-value of * $P < 0.05$.

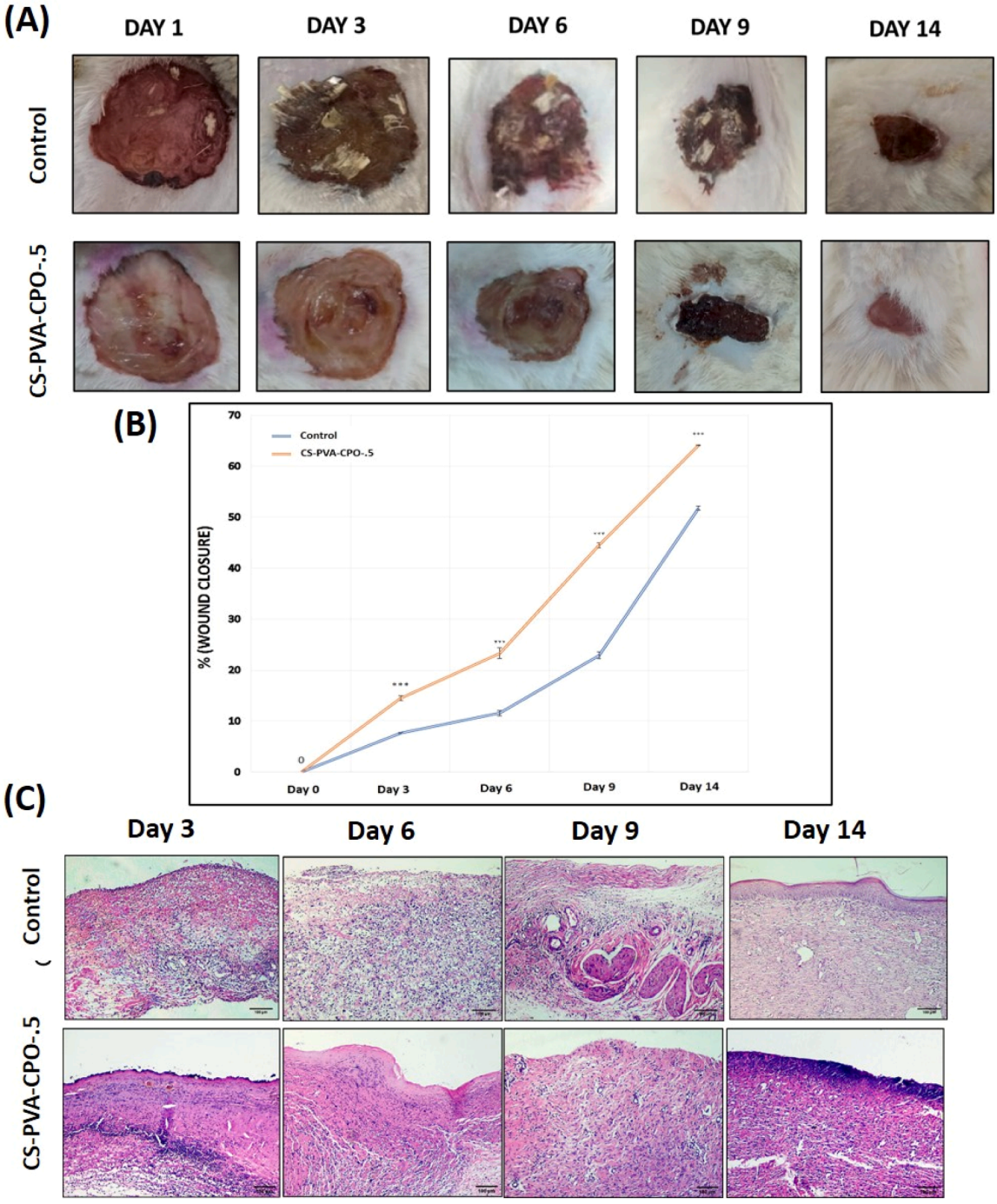

Fig. 6. Animal/In vivo studies of fabricated oxygen releasing patches using diabetic mouse model. Visual representation of wound contraction at day 1, day 3, day 6, day 9 and day 14 (A). Quantitative analysis of wound contractions over the period of 14 days (B). Histological analysis of the wound at day 3, day 6, day 9 and day 14 at 10X (C). All studies were carried out in triplicate, with a p-value of * ** $P < 0.001$.

microscope showed inflammatory cells infiltration with excessive mononuclear cells indicating evident inflammatory (phase) reaction. Furthermore, on day 6 we observed the proliferation, and neovascularization - formed blood vessels along with structured organization of wounded tissue with re-epithelization, epidermal and dermal formation. These morphological changes were more prominently noted in treated groups as compared to non-treated groups. Moreover, fibroblasts were also noted with fine distribution of collagen network as compared to untreated group that still demonstrated active inflammation at wounded site with the presence of inflammatory cells. Granulation tissue formation and remodeling was noted from day 9 to day 14 with neovascularization, reepithelization, intact epidermis and dermis formation this was more profound in treated groups as compared to untreated groups. On day 14 we noted restoration of skin architecture, tensile strength and functionality in the CS-PVA-CPO-0.5 patch treated tissue sections equivalent to normal- uninjured skin sections.

4. Conclusion

Due to insufficient nutrient and oxygen delivery to the regenerating tissue, chronic hypoxia impaired several functionalities at the wound site including lack of collagen deposition, epithelization, fibroplasia,

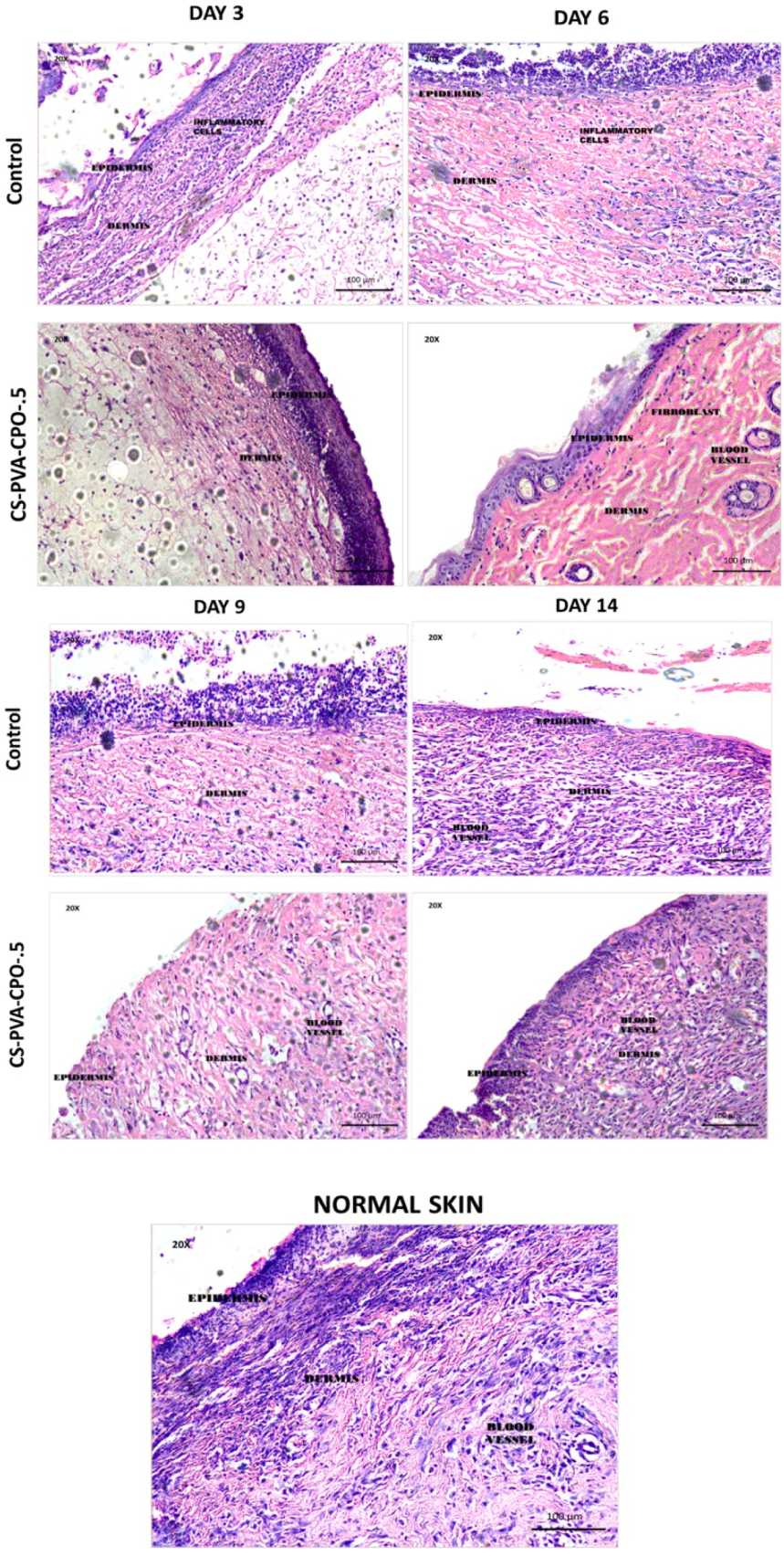

Fig. 7. Histological analysis of the wound at day 3, day 6, day 9 and day 14 at 20X magnification.

angiogenesis, and resistance to infection. Therefore, with a view to reducing hypoxia related issues, oxygen releasing CS-PVA hydrogels were prepared. Our fabricated hydrogel samples showed porous morphology indicating efficient embeddings of CPO nanoparticles inside CS-PVA hydrogels. The hydrogel's biocompatibility was proven using in vitro cell viability assays (Live/Dead and MTT assays). Furthermore, the synthesized CS-PVA hydrogels with 0.5% (w/v) CPO demonstrated excellent in vitro wound contraction capability in terms of increased fibroblast and endothelial cell migration. Furthermore, as compared to control groups on the diabetes-induced rat model, the same dosage of oxygen-releasing CS-PVA-CPO patch resulted in considerable wound contraction and accelerated wound healing. The oxygen released by oxygen generating scaffolds sustains cell viability during hypoxic conditions. HIF-1α, regulated by hypoxia and hyperglycemia, influences over 90 genes involved in angiogenesis, wound healing, proliferation, differentiation, apoptosis, and survival. Previous studies indicated increased HIF-1α expression on oxygen-releasing scaffolds [43]. Furthermore, oxygen-releasing scaffolds demonstrated enhanced angiogenic potential in chorioallantoic membrane models [43]. Additionally, hydrogen peroxide, released as an intermediate compound from CPO, exhibited improved antibacterial and antifungal activities at the wound site [44]. These combined factors significantly contribute to facilitate the healing process. Considering the findings, it can be proposed that CPO-incorporated CS-PVA hydrogel can be used to create therapeutically relevant wound healing patches that promote fast wound healing when applied to diabetic ulcers/wounds.

CRediT authorship contribution statement

Asad-Ullah: Conceptualization, Methodology, In vitro experiment, Writing-original draft, Data curation. **Abdulla Al Mamun:** Methodology, In vitro experiment, Writing- Reviewing and Editing. **MD Anwarul Hasan:** Supervision. **Midhat Batool Zaidi:** In vivo experiments, Writing- Reviewing and Editing. **Talat Roome:** Writing- Reviewing and Editing.

Declaration of Competing Interest

I am writing to confirm that the authors of the article "A Calcium peroxide incorporated Oxygen Releasing Chitosan-PVA patch for Diabetic wound healing" have no conflict of interest to declare.

Acknowledgements

This article was made possible by the NPRP12S-0310–190276 grant funded by the Qatar National Research Fund (a part of the Qatar Foundation). Funding for Open Access publication fee was provided by the Qatar National Library. We also acknowledge the support provided by the Central Laboratories Unit (CLU), Qatar University, Qatar.

Appendix A. Supporting information

Supplementary data associated with this article can be found in the online version at doi:10.1016/j.biopha.2023.115156.

References

[1] Chen, H.; Cheng, Y.; Tian, J.; Yang, P.; Zhang, X.; Chen, Y.; Hu, Y.; Wu, J. Dissolved oxygen from microalgae-gel patch promotes chronic wound healing in diabetes. Science Advances, 6, eaba4311.
[2] M. Wang, C. Wang, M. Chen, Y. Xi, W. Cheng, C. Mao, T. Xu, X. Zhang, C. Lin, W. Gao, Y. Guo, B. Lei, Efficient angiogenesis-based diabetic wound healing/skin reconstruction through bioactive antibacterial adhesive ultraviolet shielding nanodressing with exosome release, ACS Nano 13 (2019) 10279–10293.
[3] A cura di Antonio Nicolucci, Fact and figures about diabetes in Italy, Assist Inferm. Ric. 30 (2011) 100–106.
[4] M.J. Malone-Povolny, S.E. Maloney, M.H. Schoenfisch, Nitric oxide therapy for diabetic wound healing, Adv. Healthc. Mater. 8 (2019) 1801210.
[5] U.A. Okonkwo, L. Chen, D. Ma, V.A. Haywood, M. Barakat, N. Urao, L.A. DiPietro, Compromised angiogenesis and vascular Integrity in impaired diabetic wound healing, PLoS One 15 (2020), e0231962.
[6] J. Yang, Z. Chen, D. Pan, H. Li, J. Shen, Umbilical cord-derived mesenchymal stem cell-derived exosomes combined pluronic F127 hydrogel promote chronic diabetic wound healing and complete skin regeneration, Int. J. Nanomedicine. 15 (2020) 5911.
[7] H. Cho, M.R. Blatchley, E.J. Duh, S. Gerecht, Acellular and cellular approaches to improve diabetic wound healing, Adv. Drug Deliv. Rev. 146 (2019) 267–288.
[8] S.F. Spampinato, G.I. Caruso, R. De Pasquale, M.A. Sortino, S. Merlo, The treatment of impaired wound healing in diabetes: looking among old drugs, Pharm. (Basel, Switz.) (2020) *13*.
[9] S. Patel, S. Srivastava, M.R. Singh, D. Singh, Mechanistic insight into diabetic wounds: pathogenesis, molecular targets and treatment strategies to pace wound healing, Biomed. Pharmacother. 112 (2019), 108615.
[10] P.G. Rodriguez, F.N. Felix, D.T. Woodley, E.K.J.D. s Shim, The role of oxygen in wound healing: a review of the literature, Dermatol. Surg. 34 (2008) 1159–1169.
[11] D.M. Castilla, Z.-J. Liu, C. Velazquez, Oxygen: implications for wound healing, Adv. Wound Care 1 (2012) 225–230.
[12] X. Huang, P. Liang, B. Jiang, P. Zhang, W. Yu, M. Duan, L. Guo, X. Cui, M. Huang, X. Huang, Hyperbaric oxygen potentiates diabetic wound healing by promoting fibroblast cell proliferation and endothelial cell angiogenesis, Life Sci. 259 (2020), 118246.
[13] C.K. Sen, Wound healing essentials: let there be oxygen, Wound Repair Regen. 17 (2009) 1–18.
[14] R. Greif, O. Akça, E.-P. Horn, A. Kurz, D.I. Sessler, Supplemental perioperative oxygen to reduce the incidence of surgical-wound infection, N. Engl. J. Med. 342 (2000) 161–167.
[15] C.E. Fife, C. Buyukcakir, G. Otto, P. Sheffield, T. Love, R. Warriner III, Factors influencing the outcome of lower-extremity diabetic ulcers treated with hyperbaric oxygen therapy, Wound Repair Regen. 15 (2007) 322–331.
[16] M. Löndahl, P. Katzman, C. Hammarlund, A. Nilsson, M.J.D. Landin-Olsson, Relationship between ulcer healing after hyperbaric oxygen therapy and transcutaneous oximetry, toe blood pressure and ankle-brachial index in patients with diabetes and chronic foot ulcers, Diabetologia 54 (2011) 65–68.
[17] C.L.J.J. o v Broussard, N. Hyperb. Oxyg. Wound Heal. 22 (2004) 42–48.
[18] K.M. Fosen, S.R. Thom, Hyperbaric oxygen, vasculogenic stem cells, and wound healing, Antioxid. Redox. Signal. 21 (2014) 1634–1647.
[19] M. Löndahl, Hyperbaric oxygen therapy as adjunctive treatment for diabetic foot ulcers, Int. J. Low. Extrem. Wounds 12 (2013) 152–157.
[20] C.-Y. Chen, R.-W. Wu, M.-C. Hsu, C.-J. Hsieh, M.-C. Chou, W. Ostomy, C. Nursing, Adjunctive hyperbaric oxygen therapy for healing of chronic diabetic foot ulcers: a randomized controlled trial, J. Wound. Ostomy. Continence. Nurs . 44 (2017) 536–545.
[21] Kranke, P.; Bennett, M.H.; Martyn-St James, M.; Schnabel, A.; Debus, S.E.; Weibel, S. Hyperbaric oxygen therapy for chronic wounds. 2015.
[22] M. Heyboer III, D. Sharma, W. Santiago, N.J.A. McCulloch, Hyperbaric oxygen therapy: side effects defined and quantified, Adv. Wound Care. 6 (2017) 210–224.
[23] S. Opasanon, W. Pongsapich, S. Taweepraditpol, B. Suktitipat, A. Chuangsuwanich, Clinical effectiveness of hyperbaric oxygen therapy in complex wounds, J. Am. Coll. Clin. Wound Spec. 6 (2014) 9–13.
[24] H.W. Hopf, J.J. Gibson, A.P. Angeles, J.S. Constant, J.J. Feng, M.D. Rollins, M. Zamirul Hussain, T.K. Hunt, Hyperoxia and angiogenesis, Wound Repair Regen. 13 (2005) 558–564.
[25] A.L. Farris, A.N. Rindone, W.L. Grayson, Oxygen delivering biomaterials for tissue engineering, J. Mater. Chem. B 4 (2016) 3422–3432.
[26] S. Suvarnapathaki, X. Wu, D. Lantigua, M.A. Nguyen, G. Camci-Unal, Breathing life into engineered tissues using oxygen-releasing biomaterials, NPG Asia Mater. 11 (2019), 65-65.
[27] Z. Li, X. Guo, J.J.B. Guan, An oxygen release system to augment cardiac progenitor cell survival and differentiation under hypoxic condition 33 (2012) 5914–5923.
[28] G. Camci-Unal, N. Alemdar, N. Annabi, A.J.P. i Khademhosseini, Oxygen releasing biomaterials for tissue engineering, Polym. Int. 62 (2013) 843–848.
[29] C.-S. Yeh, R. Wang, W.-C. Chang, Y.-h J.J. o e m Shih, Synthesis and characterization of stabilized oxygen-releasing CaO2 nanoparticles for bioremediation, J. Environ. Manag. 212 (2018) 17–22.
[30] L. Daneshmandi, C.T.J.J. o B.M.R.P.A. Laurencin, Regenerative engineered vascularized bone mediated by calcium peroxide 108 (2020) 1045–1057.
[31] H. Wang, Y. Zhao, T. Li, Z. Chen, Y. Wang, C. Qin, Properties of calcium peroxide for release of hydrogen peroxide and oxygen: A kinetics study, Chem. Eng. J. 303 (2016) 450–457.
[32] F. Jiang, Y. Zhang, G.J.J.P. r Dusting, NADPH oxidase-mediated redox signaling: roles in cellular stress response, stress tolerance, and tissue repair, Pharmacol. Rev. 63 (2011) 218–242.
[33] M. Aleemardani, A. Solouk, S. Akbari, M.M. Dehghan, M. Moeini, Silk-derived oxygen-generating electrospun patches for enhancing tissue regeneration: investigation of calcium peroxide role and its effects on controlled oxygen delivery, Materialia 14 (2020), 100877.
[34] H. Cheng, Z. Shi, K. Yue, X. Huang, Y. Xu, C. Gao, Z. Yao, Y.S. Zhang, J. Wang, Sprayable hydrogel dressing accelerates wound healing with combined reactive oxygen species-scavenging and antibacterial abilities, Acta Biomater. 124 (2021) 219–232.
[35] N. Akhavan-Kharazian, H. Izadi-Vasafi, Preparation and characterization of chitosan/gelatin/nanocrystalline cellulose/calcium peroxide films for potential wound dressing applications, Int. J. Biol. Macromol. 133 (2019) 881–891.

[36] K. Kalantari, E. Mostafavi, B. Saleh, P. Soltantabar, T.J. Webster, Chitosan/PVA hydrogels incorporated with green synthesized cerium oxide nanoparticles for wound healing applications, Eur. Polym. J. 134 (2020), 109853.
[37] X. Feng, X. Hou, C. Cui, S. Sun, S. Sadik, S. Wu, F. Zhou, Mechanical and antibacterial properties of tannic acid-encapsulated carboxymethyl chitosan/polyvinyl alcohol hydrogels, Eng. Regen. 2 (2021) 57–62.
[38] C. Alvarez-Lorenzo, A. Concheiro, Reversible adsorption by a pH- and temperature-sensitive acrylic hydrogel, J. Contr. Release 80 (2002) 247–257.
[39] Y. Tang, Y. Du, Y. Li, X. Wang, X. Hu, A thermosensitive chitosan/poly(vinyl alcohol) hydrogel containing hydroxyapatite for protein delivery, J. Biomed. Mater. Res. A 91 (2009) 953–963.
[40] A.A. Zahid, R. Augustine, Y.B. Dalvi, K. Reshma, R. Ahmed, S. Raza ur Rehman, H. E. Marei, R. Alfkey, A. Hasan, Development of nitric oxide releasing visible light crosslinked gelatin methacrylate hydrogel for rapid closure of diabetic wounds, Biomed. Pharmacother. 140 (2021), 111747.
[41] Z. Xu, S. Han, Z. Gu, J.J.A. h m Wu, Advances and Impact of Antioxidant Hydrogel in Chronic Wound Healing, Wiley, 2020, 1901502.
[42] T. Agarwal, S. Kazemi, M. Costantini, F. Perfeito, C.R. Correia, V. Gaspar, L. Montazeri, C. De Maria, J.F. Mano, M. Vosough, P. Makvandi, T.K. Maiti, Oxygen releasing materials: towards addressing the hypoxia-related issues in tissue engineering, Mater. Sci. Eng.: C. 122 (2021), 111896.
[43] M. Zehra, W. Zubairi, A. Hasan, H. Butt, A. Ramzan, M. Azam, A. Mehmood, M. Falahati, A. Anwar Chaudhry, I. Ur Rehman, M. Yar, Oxygen generating polymeric nano fibers that stimulate angiogenesis and show efficient wound healing in a diabetic wound model, Int. J. Nanomed. 15 (2020) 3511–3522.
[44] A. Fadakar Sarkandi, M. Montazer, M. Mahmoudi Rad, Oxygenated-bacterial-cellulose nanofibers with hydrogel, antimicrobial, and controlled oxygen release properties for rapid wound healing, Wiley, 2022, 51974.